

Cite this article as: Qiao Xudong, Chen Minghe, Xie Lansheng. Deep Drawing and Gas Bulging of Precise Hot Forming Process of Complex Box Part[J]. Rare Metal Materials and Engineering, 2024, 53(06): 1582-1591. DOI: 10.12442/j.issn.1002-185X.20230472.

ARTICLE

Deep Drawing and Gas Bulging of Precise Hot Forming Process of Complex Box Part

Qiao Xudong, Chen Minghe, Xie Lansheng

College of Mechanical & Electrical Engineering, Nanjing University of Aeronautics and Astronautics, Nanjing 210016, China

Abstract: In order to solve the problems of insufficient forming of complex box part in the single deep drawing, a precise hot forming process of deep drawing and gas bulging was proposed, and the shape and thickness of the formed parts could meet the design requirements. TC2 titanium alloy complex box part was selected as the research object in this research. The high temperature formability of TC2 titanium alloy was investigated at 550–800 °C and 0.001–0.1 s⁻¹. A set of mold for deep drawing and gas bulging at one time was designed. The forming process of the complex box part was simulated based on the finite element simulation software PAM-STAMP, and the optimized process parameters were obtained and verified by experiments. Results show that the simulation software PAMSTAMP can effectively predict the part defects during deep drawing and gas bulging. The process parameters and mold shape are ameliorated and verified by experiments. Complex box part with thickness and height meeting the design requirements can be obtained under the conditions of 800 °C and gas pressure of 2.5 MPa, which verifies the feasibility of the composite process of deep drawing and gas bulging.

Key words: TC2 titanium alloy; high temperature rheological properties; composite process; numerical simulation

Titanium alloy is an excellent metal material with high strength, low density, and high service temperature, which is widely used in the manufacture of aerospace high-strength lightweight structural parts, such as aircraft sheet metal components, aircraft skin, engine fairing, fan blades, and missile parts. Due to their poor plasticity and large springback at room temperature, titanium alloy parts with high shape precision are often processed by hot forming to enhance their plasticity. However, complex titanium alloy parts with irregular shapes cannot be achieved by simple hot forming process. For example, TC2 complex box part in the engine has a high degree of flanging and a large degree of bending, so it inevitably cracks after single hot deep drawing process. Single-drawing or multi-pass drawing methods are often used to form cylindrical or box-shaped parts^[1-4]. The hot drawing process can improve the plasticity of materials, thereby enhancing the formability of the parts. Multi-pass hot deep drawing process can significantly reduce the defects of parts, such as cracking and thinning, but more drawing molds are required. Moreover, the parts undergoing several plastic

deformation need to be annealed to release residual stress, so its service life decreases, which leads to complex processes, high cost, and low production efficiency^[5]. As a flexible sheet metal forming process, hydroforming process replaces the mold with hydraulic oil or other liquid media, which can well avoid the problems of insufficient workpiece forming in traditional deep drawing^[6]. However, this process requires not only a large-tonnage hydraulic press but also an independent closed-loop control system, resulting in even higher production cost. Therefore, it is urgent to investigate a new forming process to improve the forming quality and production efficiency of complex box parts.

In recent years, superplastic gas bulging forming has become more and more popular in the deep drawing field for sheet metals^[7]. This method uses gas instead of rigid die to form parts with complex shapes, which takes advantage of the low stress and high plasticity of materials at the certain temperature and strain rate. Fu et al^[8] formed thin-wall bending tube of TC4 titanium alloy by hot gas bulging process. The forming accuracy and wall thickness uniformity

Received date: July 30, 2023

Foundation item: National Natural Science Foundation of China (52375345)

Corresponding author: Chen Minghe, Ph. D., Professor, College of Mechanical & Electrical Engineering, Nanjing University of Aeronautics and Astronautics, Nanjing 210016, P. R. China, E-mail: meemhchen@nuaa.edu.cn

Copyright © 2024, Northwest Institute for Nonferrous Metal Research. Published by Science Press. All rights reserved.

of thin-wall bending tube are improved by controlling the main process parameters, such as forming temperature and strain rate. Xu et al^[9] used the rapid superplastic process combined with hot stamping and superplastic gas bulging to form high-speed iron skin parts with the wall thickness thinning ratio of 25%, and the forming accuracy and mechanical properties met the technical requirements. Zhou et al^[10] used the finite element method to analyze the wall thickness distribution of Ti-55 titanium alloy double-layer plate formed under superplastic conditions and adjusted the gas loading path to control the process. The wall thickness difference between the numerical simulation results and the experiment results is small, and the average relative error is 5.87%. Hu et al^[11] heated the Al-Mg alloy sheet to 450 °C for 15 min, then inflated the square pyramid-shaped part, and expanded the part under the pressure of 2 MPa. It is found that the tensile strength and hardness of the formed parts are increased with the increase in deformation, which indicates that hot gas bulging with clustering balls method can improve the formability and mechanical properties of the formed parts.

Therefore, in order to improve the forming quality of complex box parts and to increase the production efficiency, a composite hot forming process combining deep drawing and gas bulging was proposed in this research. In the deep drawing process, the blank was at the three-way complex stress state in the flange deformation region and punch corner area. The blank deformation is not uniform, the part is prone to wrinkle when the shear stress is too large, and the bottom fillet is prone to crack when the tensile stress is too large. The blank is at the biaxial tensile stress state in the gas bulging forming process, and the deformation is obviously different due to different forces in each area during the forming process, resulting in uneven thickness of formed parts^[12]. In this research, by controlling the process ratio of deep drawing and gas bulging, the drawing process was ceased before the parts break and wrinkle, and the gas bulging process was used to form the final part shape.

The influence of temperature and forming speed on the formability of TC2 titanium alloy was investigated, and the stress-strain curve of TC2 titanium alloy at high temperature was obtained. PAM-STAMP finite element software was used to simulate the hot deep drawing and gas bulging process, and the process proportion of deep drawing to gas bulging was discussed. The process parameters were determined, the mold shape was optimized, and the verification experiment was conducted.

1 Experiment

TC2 titanium alloy is nearly α -type at room temperature^[13] with close-packed hexagonal lattice structure, which only has three slip systems and poor plasticity at room temperature. The plastic deformation ability is usually affected by deformation temperature and strain rate^[14]. Therefore, it is necessary to conduct high temperature tensile experiments of TC2 titanium alloy to obtain their high temperature

mechanical properties and provide data support for part forming. The experiment parts were prepared by TC2 titanium alloy hot-rolled sheet with thickness of 2 mm in this research, and the main chemical composition of TC2 titanium alloy is shown in Table 1.

The tensile sample was cut according to ASTM E2448 standard with 25.4 mm in gauge length. The schematic diagram of tensile sample is shown in Fig. 1. The high temperature tensile tests were conducted at the temperatures of 550, 600, 650, 700, 750, and 800 °C and strain rates of 0.1, 0.01, and 0.001 s⁻¹ by UTM5504X electronic universal testing machine, which accompanied by a high temperature furnace with control accuracy of ± 2 °C. Three groups of experiments were conducted under each experiment condition to ensure the result accuracy, and 54 sets of experiments were conducted. The measurement errors for both stress and strain values were within $\pm 0.5\%$. Before the experiment, the gauge section of each sample was carefully polished to avoid the influence of stress concentration caused by burrs and scratches on the sample surface. Then, the sample was put into the holding furnace and heated for 15 min.

The composite hot forming process of hot drawing and gas bulging was conducted through the 150-ton frame hot forming machine. The machine system included a pneumatic control system, a temperature control system, a hydraulic control system, and a solenoid valve PLC control system. A set of mold for deep drawing and gas bulging was designed, and the hot drawing process was completed by pressure equipment with 12 separate heating zones and temperature controllers. The gas bulging forming process was conducted by the gas cylinder and pressure control cabinet, which was controlled by software to adjust pressure loading and to monitor the gas pressure during the forming process in real time.

2 High Temperature Rheological Properties

2.1 High temperature rheological characteristics

Fig. 2 shows the true stress-true strain curves of TC2 titanium alloy at different high temperatures. In the early stage of tensile deformation at high temperature, the rapid increase in dislocation density causes the work hardening effect of TC2 titanium alloy, and the true stress is increased rapidly with the increase in true strain. When the deformation exceeds a

Table 1 Chemical composition of TC2 titanium alloy (wt%)

Al	Mn	Fe	O	C	H	N	Ti
4.0	1.67	0.03	0.1	0.006	0.0025	0.004	Bal.

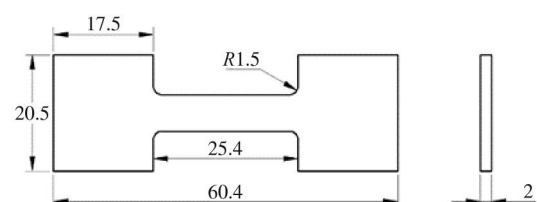


Fig.1 Schematic diagram of high temperature tensile sample

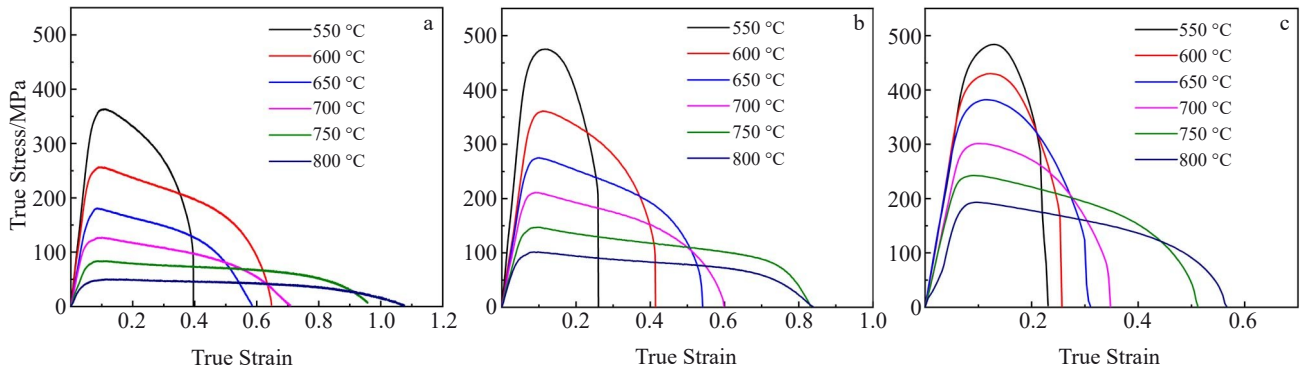


Fig.2 True stress-true strain curves of TC2 titanium alloy at different high temperatures under strain rate of 0.1 s^{-1} (a), 0.01 s^{-1} (b), and 0.001 s^{-1} (c)

certain value, the work hardening and dynamic softening effects reach a balance, the flow stress reaches the peak value, and the TC2 titanium alloy enters the steady flow stage. With the increase in deformation degree, the plastic deformation stage is started, and the stress is gradually decreased until the tensile sample breaks^[15-16]. Under the same strain rate, with the increase in temperature, the peak stress is decreased, and the elongation is increased firstly, then decreased, and finally increased. At the same temperature, with the decrease in strain rate, the peak stress is decreased and the maximum elongation is increased. At 800 °C and 0.001 s^{-1} , the minimum peak stress and maximum elongation are 50.5 MPa and 212.5% , respectively. The experiment results of mechanical properties of TC2 titanium alloy at different temperatures under strain rate of 0.001 s^{-1} are shown in Table 2.

2.2 Constitutive model

The constitutive equation of TC2 titanium alloy is influenced by many factors, such as strain, strain rate, and temperature^[17]. In this research, the temperature and strain rate of TC2 titanium alloy were tested at the same time. Considering the change in temperature and strain rate, the hyperbolic sinusoidal Arrhenius constitutive model was adopted to express the relationship between flow stress and strain rate at different temperatures. The specific equations are as follows^[18]:

$$\dot{\epsilon} = A \sinh(\alpha\sigma)^n \exp(-Q/RT) \quad \forall \alpha\sigma \quad (1)$$

$$\dot{\epsilon} = A_1 \sigma^{n_1} \exp(-Q/RT) \quad \alpha\sigma < 0.8 \quad (2)$$

$$\dot{\epsilon} = A_2 \exp(\beta\sigma) \exp(-Q/RT) \quad \beta\sigma > 1.2 \quad (3)$$

where $\dot{\epsilon}$ is the strain rate in s^{-1} ; Q is the thermal deformation activation energy in $\text{kJ}\cdot\text{mol}^{-1}$; R is the gas constant of

$8.314 \text{ mol}^{-1}\cdot\text{K}^{-1}$; σ is the true stress in MPa ; T is the temperature in K ; A , A_1 , A_2 , α , β , n , and n_1 are material-related parameters and $\beta = \alpha n_1$.

In order to analyze the influence of temperature and strain rate on the rheological properties of TC2 titanium alloy, Z parameter was introduced, and its specific form is as follows:

$$Z = \dot{\epsilon} \exp(Q/RT) \quad (4)$$

Taking logarithms of both sides of Eq.(1-3), Eq.(5-7) can be obtained, respectively, as follows:

$$\ln[\sinh(\alpha\sigma)] = \frac{1}{n} \ln \dot{\epsilon} - \frac{1}{n} \ln A + \frac{Q}{nRT} \quad (5)$$

$$\ln \sigma = \frac{1}{n_1} \ln \dot{\epsilon} - \frac{1}{n_1} \ln A_1 + \frac{1}{n_1} \frac{Q}{RT} \quad (6)$$

$$\sigma = \frac{1}{\beta} \ln \dot{\epsilon} - \frac{1}{\beta} \ln A_2 + \frac{1}{\beta} \frac{Q}{RT} \quad (7)$$

Taking $\ln \sigma$ and σ as the dependent variables and $\ln \dot{\epsilon}$ as the independent variable, the data points were taken into Eq.(6) and Eq.(7) to draw $\ln \sigma - \ln \dot{\epsilon}$ and $\sigma - \ln \dot{\epsilon}$ fitting lines with the slopes of $1/n_1$ and $1/\beta$ at true strain $\epsilon=0.2$, as shown in Fig.3a and 3b, respectively. Through the average slopes of fitting line, $n_1=5.384$, $\beta=0.032$, and $\alpha=0.006 \text{ MPa}^{-1}$. Similarly, the slopes of $\ln[\sinh(\alpha\sigma)] - \ln \dot{\epsilon}$ and $\ln[\sinh(\alpha\sigma)] - 1/T$ fitting lines are $1/n$ and Q/nR , as shown in Fig.3c and 3d, respectively. Therefore, the thermal deformation activation energy Q of TC2 titanium alloy is as follows:

$$Q = R \frac{\partial \ln \dot{\epsilon}}{\partial \ln[\sinh(\alpha\sigma)]} \frac{\partial \ln[\sinh(\alpha\sigma)]}{\partial (1/T)} = R\gamma\theta \quad (8)$$

According to the linear fitting results, the substitution symbols $\gamma=3.969$ and $\theta=77604.13$, leading to the thermal deformation activation energy $Q=250.945 \text{ kJ}\cdot\text{mol}^{-1}$.

Table 2 Mechanical properties of TC2 titanium alloy at different temperatures under strain rate of 0.001 s^{-1}

Temperature/ $^{\circ}\text{C}$	Yield strength/ MPa	Tensile strength/ MPa	Elongation/ $\%$
550	288.3	363.7	56.9
600	212.6	256.4	104.4
650	143.2	180.4	87.8
700	111.3	126.8	117.2
750	71.4	84.1	174.9
800	36.1	50.5	212.5

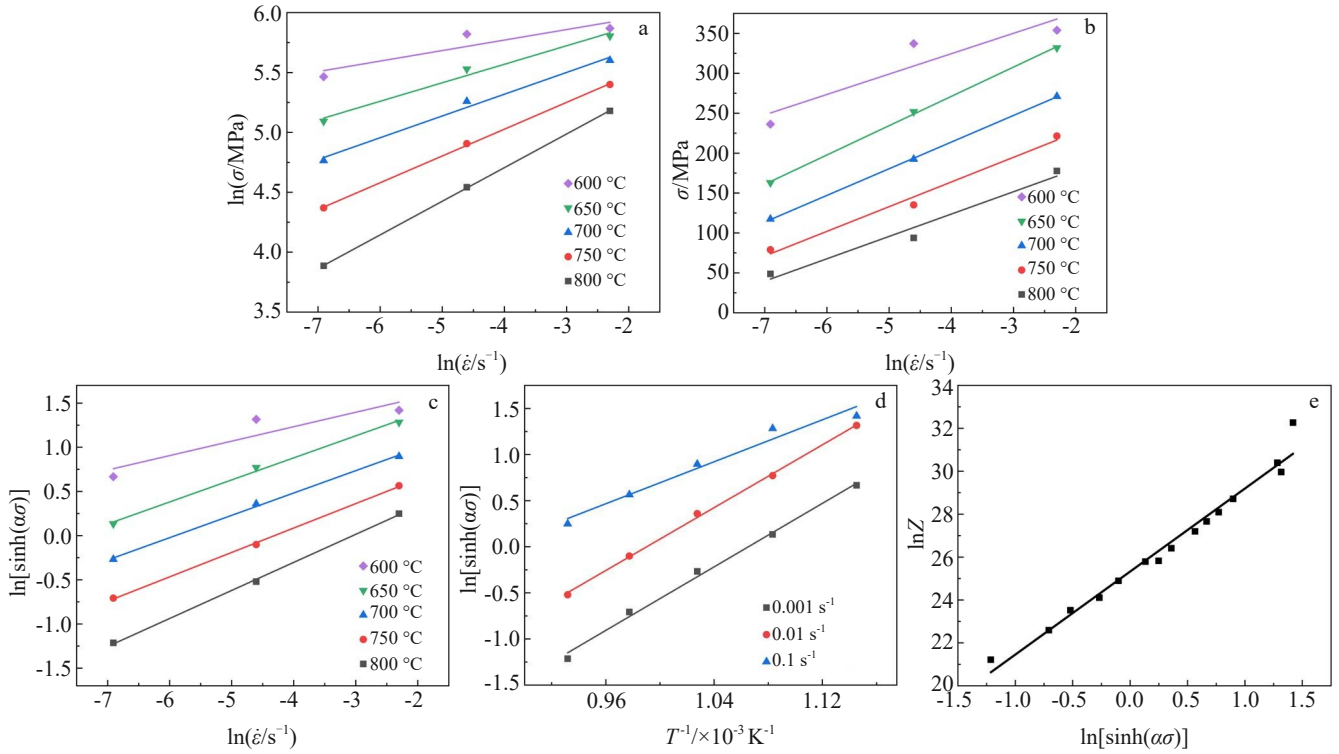


Fig.3 Fitting lines of $\ln\sigma\text{-}\ln\dot{\epsilon}$ (a), $\sigma\text{-}\ln\dot{\epsilon}$ (b), $\ln[\sinh(\alpha\sigma)]\text{-}\ln\dot{\epsilon}$ (c), $\ln[\sinh(\alpha\sigma)]\text{-}1/T$ (d), and $\ln Z\text{-}\ln[\sinh(\alpha\sigma)]$ (e) at true strain $\epsilon=0.2$

Taking the derivative of both sides of Eq. (1), the fitting lines of $\ln Z\text{-}\ln[\sinh(\alpha\sigma)]$ can be obtained, as shown in Fig.3e. The obtained equation coefficients are $n=3.87$ and $\ln A=25.3254$.

In summary, the Arrhenius constitutive model of TC2 titanium alloy at true strain $\epsilon=0.2$ can be expressed as follows:

$$\sigma = \frac{1}{0.006} \ln \left\{ \left(\frac{Z}{9.97 \times 10^{10}} \right)^{\frac{1}{3.87}} + \left[\left(\frac{Z}{9.97 \times 10^{10}} \right)^{\frac{2}{3.87}} + 1 \right]^{\frac{1}{2}} \right\} \quad (9)$$

$$Z = \dot{\epsilon} \exp \left(\frac{250.945 \times 10^3}{8.314T} \right) \quad (10)$$

The relevant parameters in Eq.(9–10) are shown in Table 3 and Table 4.

Since the traditional Arrhenius constitutive model cannot reflect the relationship between strain and stress, the strain compensation was introduced in this study. The material parameters of Arrhenius constitutive model under the strain variables of 0.1, 0.15, 0.2, 0.25, and 0.3 were calculated. Taking α , Q , n , and $\ln A$ as the dependent variables and strain as the independent variable, the fitting of quintic polynomial was conducted. The fitting equations

are as follows:

$$\begin{cases} \alpha(\epsilon) = -42.69\epsilon^5 + 24.1\epsilon^4 - 2.777\epsilon^3 - 0.4524\epsilon^2 + 0.1071\epsilon \\ Q(\epsilon) = 8.245 \times 10^8 \epsilon^5 - 8.321 \times 10^8 \epsilon^4 + 3.483 \\ \quad \times 10^8 \epsilon^3 - 7.042 \times 10^7 \epsilon^2 + 6.744 \times 10^6 \epsilon \\ n(\epsilon) = 26520\epsilon^5 - 24730\epsilon^4 + 8871\epsilon^3 - 1499\epsilon^2 + 119.7\epsilon \\ \ln A(\epsilon) = 97660\epsilon^5 - 90930\epsilon^4 + 36020\epsilon^3 - 7098\epsilon^2 + 676.5\epsilon \end{cases} \quad (11)$$

In order to evaluate the accuracy of the quintic polynomial correlation, coefficient R and absolute average relative error (AARE) were used to calculate and to analyze the accuracy of the model, as follows:

$$R = \frac{\sum_{i=1}^N (C_i - \bar{C})(P_i - \bar{P})}{\sqrt{\sum_{i=1}^N (C_i - \bar{C})^2 (P_i - \bar{P})^2}} \quad (12)$$

$$\text{AARE} = \frac{1}{N} \sum_{i=1}^N |(C_i - P_i)/C_i| \quad (13)$$

where C_i is the experimental stress in MPa, \bar{C} is the average of experimental stress in MPa, P_i is the predicted stress in MPa, \bar{P} is the average of predicted stress in MPa, and N is the number of samples.

The correlations between calculated σ results of Arrhenius constitutive model and experimental σ results with strain

Table 3 Relevant parameters of established Arrhenius constitutive model at true strain $\epsilon=0.2$ and different temperatures

Parameter	600 °C	650 °C	700 °C	750 °C	800 °C	Mean
n_1	11.3986	6.4708	5.5001	4.4691	3.5608	6.2799
β	0.0391	0.0272	0.0299	0.0323	0.0357	0.0328
α	0.0034	0.0042	0.0054	0.0072	0.0100	0.0060
γ	6.1180	4.0077	3.9551	3.9189	3.1495	4.2298

Table 4 Relevant parameters of established Arrhenius constitutive model at true strain $\varepsilon=0.2$ and different strain rates

Parameter	0.001 s ⁻¹	0.01 s ⁻¹	0.1 s ⁻¹	Mean
θ	8607.01	8516.41	5688.98	7604.13
n	-	-	-	3.87
$\ln A$	-	-	-	25.3254

compensation in the range of true strain as 0.1–0.3 are shown in Fig.4. The correlation coefficient R is equal to 0.9934 and AARE is equal to 5.306%, which indicates that the error of prediction results of this model is small. In conclusion, the Arrhenius constitutive model based on strain compensation is accurate for the flow stress prediction of TC2 titanium alloy with the true strain range as 0.1–0.3. The relative error with the simulated forming part is only 3.59%.

2.3 Hardening model

In order to describe the hardening behavior of TC2 titanium alloy, Hollomon strain hardening model was established and used in PAM-STAMP simulation software^[19], and its expression^[20] is as follows:

$$\sigma = K\varepsilon^n \quad (14)$$

where σ is the true stress (MPa), K is the strengthening factor, ε is the true plastic strain, and n is the tensile strain hardening exponent. The exponential equation is transformed into a logarithmic equation, as follows:

$$\ln \sigma = n \ln \varepsilon + \ln K \quad (15)$$

If $y=\ln\sigma$, $A=n$, $x=\ln\varepsilon$, and $B=\ln K$, $y=Ax+B$ can be obtained. Five points at the uniform plastic deformation stage of the tensile curve of the material were calculated to obtain the relational expression of strain hardening index n , as follows:

$$n = \frac{5 \sum_{i=1}^5 x_i y_i - \sum_{i=1}^5 x_i \sum_{i=1}^5 y_i}{5 \sum_{i=1}^5 x_i^2 - (\sum_{i=1}^5 x_i)^2} \quad (16)$$

Finally, the strengthening factor K and strain hardening exponent n under each experiment condition are obtained, as shown in Table 5.

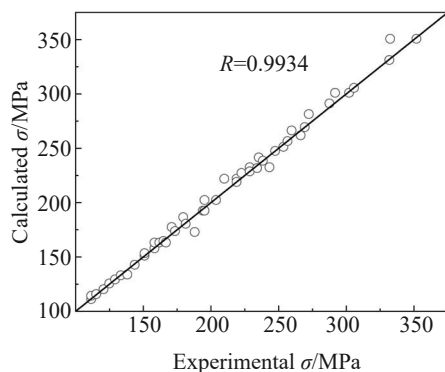


Fig.4 Correlation between calculated σ results by Arrhenius constitutive model and experimental σ results

Table 5 Parameters of Hollomon hardening model under different experiment conditions

Temperature/ °C	Strain rate/ s ⁻¹	Strengthening factor, K	Strain hardening exponent, n
550	0.1	338.49	0.1402
	0.01	308.24	0.1856
	0.001	247.87	0.1596
600	0.1	274.42	0.1869
	0.01	241.77	0.1676
	0.001	173.29	0.1780
650	0.1	206.46	0.2640
	0.01	155.39	0.2547
	0.001	101.59	0.2632
700	0.1	172.39	0.2538
	0.01	128.26	0.2259
	0.001	56.78	0.4132
750	0.1	172.41	0.1566
	0.01	84.84	0.2556
	0.001	59.19	0.1494
800	0.1	120.49	0.2062
	0.01	59.38	0.2528
	0.001	31.02	0.1966

3 Process and Finite Element Analysis

3.1 Part structure analysis

The part structure is shown in Fig. 5. The total width is 46 ± 0.8 mm, the total length is 66 mm, the depth is 18 ± 0.8 mm, and the thickness of the part is 2 mm.

The forming difficulty results from the asymmetrical shape on both sides of the X axis and the drawing angle is about 110° . The side height of part should be greater than 18 mm, the bottom surface and side of the part are easy to wrinkle, the rounded corner may break, and the maximum thinning ratio of the formed part cannot be greater than 25%.

3.2 Composite process design

For the preparation of complex box part of TC2 titanium alloy, a composite hot forming process of deep drawing and gas bulging was developed in this research. This process uses the same set of mold to complete two processes, including the deep drawing and the gas bulging forming. It can avoid part cracking and wrinkling caused by large deformation in single forming. The blank and mold are enlarged in order to use one mold to form two parts, thereby improving the production efficiency.

3.3 Finite element model

PAM-STAMP software was used for the finite element

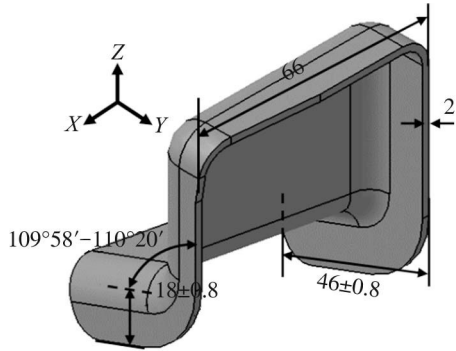


Fig.5 Schematic diagram of TC2 titanium alloy complex box part

simulation of the complex box part. In order to simplify the finite element model, the simulation process was set in an isothermal environment without considering the temperature field changes caused by possible temperature differences in the actual process^[21]. Mold and blank model were designed in CATIA V5R21 software, and then they were imported into PAM-STAMP software in IGES format. The mesh type was C3D4. The blank mesh size was 4 mm×4 mm, the maximum mold mesh size was set as 14 mm, and the mesh refinement level was set as 3 mm. The material parameters were obtained from the tensile test results at high temperature. Poisson ratio μ was set as 0.3, density ρ was set as 4.55 g·cm⁻³, and the thickness of blank was set as 2 mm. Fixed constraints were applied to the die, displacement constraints were applied to the punch, and the finite element model was established, as shown in Fig.6.

3.4 Simulation results and discussion

Firstly, the proportion of deep drawing process in composite forming process was studied to explore the feasibility of the composite process. Normally, the deep drawing often leads to the cracks. Therefore, a pre-deep

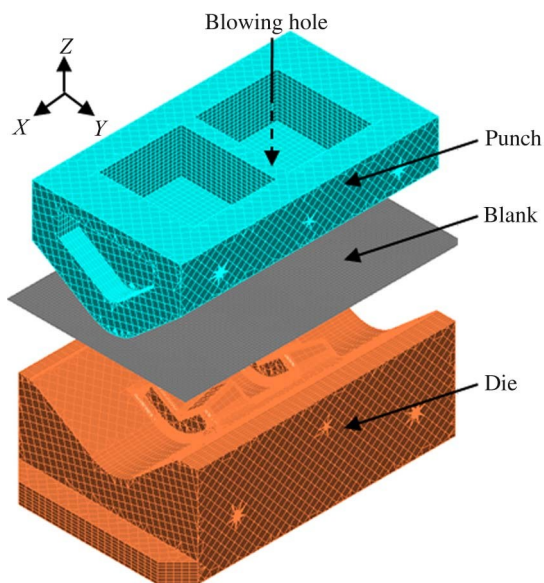


Fig.6 Schematic diagram of finite element assembly model

drawing method was employed to prevent the crack formation. The punch displacement was controlled to draw to 40%, 60%, and 80% of the final part height, as shown in Fig. 7a. The minimum thickness of blank at 700 °C is decreased with the increase in the deep drawing ratio. The bottom of the part is basically formed when the depth reaches 80%. At this time, the minimum thickness at the round corner is 1.597 mm, the thinning ratio is about 20%, and the thickness of the main forming area is even. With the drawing process further proceeding, the maximum thinning ratio is close to 25%, and the part may risk the crack formation^[22]. Since deep drawing offers higher production efficiency, compared with gas bulging in forming processes, it is conducive to increase the deep drawing ratio as much as possible. Deep drawing to 80% of the final part height not only allows for the formation of a defined part shape without significant defects, but also ensures the sufficient deformation allowance for subsequent gas bulging process.

After determining the deep drawing ratio, the simulation of the gas bulging process was conducted. Fig. 7b shows the simulation results of the gas bulging forming under different pressures at 700 °C. When the pressure is between 0.5 and 1.5 MPa, the parts cannot be fully formed due to insufficient pressure. At the pressure of 2.5 MPa, the part can be well formed, demonstrating the feasibility of the composite hot forming process. However, at this stage, the maximum thinning ratio of the part approaches 70%. This may be due to the insufficient plasticity of TC2 titanium alloy at 700 °C, or the excessive gas pressure, which leads to severe thinning

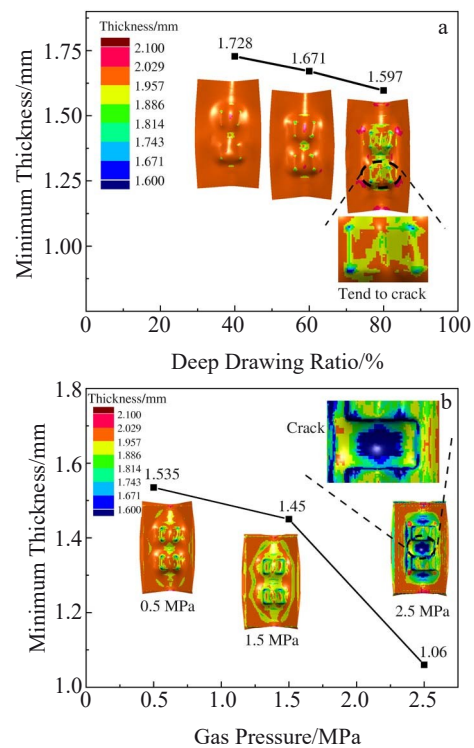


Fig.7 Simulation results of deep drawing (a) and gas bulging (b) processes at 700 °C

phenomenon in the primary forming area. Therefore, although the composite hot forming process is feasible, the temperature of 700 °C is not suitable for part formation. It is necessary to further discuss the impact of gas pressure and forming temperature on the part formation.

According to the high temperature tensile test results of TC2 titanium alloy, the flow stress significantly reduces when the temperature is greater than 750 °C, and the deformation resistance is very small, which is conducive to the material flow. According to Fig. 7b, the part can be fully formed when the gas pressure reaches 2.5 MPa. However, considering the production cost, the process pressure is expected to be less than 2 MPa, which can be achieved by increasing the temperature and improving the material flow performance. Therefore, the parameters of simulation analysis were selected as temperature of 750 and 800 °C and gas pressure of 2 and 2.5 MPa. Table 6 shows four different experimental schemes.

Simulation analysis of composite hot forming process of

Table 6 Simulation test schemes

No.	Temperature/°C	Gas pressure/MPa	Depth of drawing
1	750	2	80%
2	750	2.5	
3	800	2	
4	800	2.5	

deep drawing and gas bulging was conducted and the results are shown in Fig. 8. The results of No. 1–No. 3 tests show that the part is not completely formed. Only when the temperature reaches 800 °C, the maximum thinning ratio of the part reaches 67%, which means the crack formation.

With the increase in the forming temperature, the yield strength of TC2 titanium alloy is decreased, the plasticity is enhanced, and the deformation resistance is significantly reduced. However, at this stage, the gas pressure of 2 MPa is insufficient for part formation, whereas the gas pressure of 2.5 MPa leads to severe thinning of the part. Therefore, it is essential to consider the impact of the gas pressure loading path on the results of gas bulging forming.

In the process of gas bulging forming, excessive initial gas pressure will cause high strain rate in the local areas, resulting in severe thinning and cracking^[23]. Therefore, considering the influence of pressure loading rate on blank material flow, a slow step pressure loading path was adopted to improve the plasticity of the material^[24]. Compared with the original gas loading path, the forming pressure is low at the early stage with the slow loading path. When the blank material continues to get close to the die, the pressure increases, promoting the formation of corners and sides of the part. Two loading paths are compared and the results are shown in Fig. 9. The simulation results with slow loading path at different temperatures are shown in Fig. 10. Obviously, the slow pressure loading path can improve the thinning problem in Fig. 8d. The thinning problem of the formed part is well settled

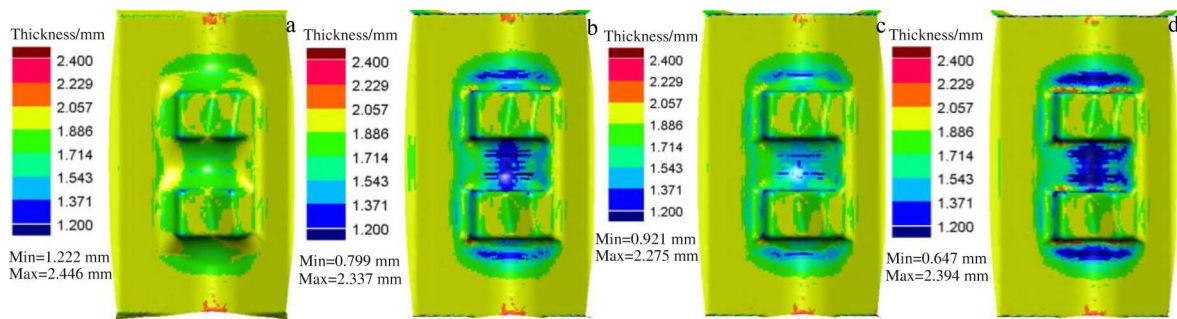


Fig. 8 Simulation results of No.1 (a), No.2 (b), No.3 (c), and No.4 (d) tests

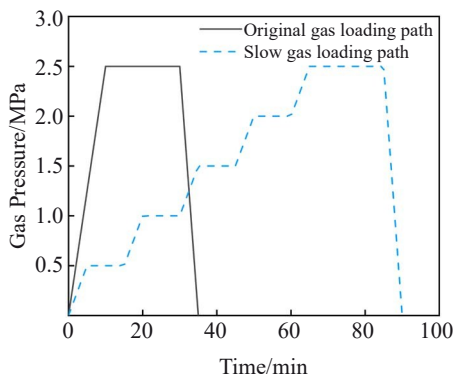


Fig. 9 Comparison of original and slow gas loading paths

at 800 °C, but the maximum thinning ratio is still more than 25%. The change in pressure or temperature has a little effect at this time, and the optimization of the die is considered to solve the problems of thinning and insufficient shape forming.

To shrink the blank towards the rounded corner during the gas bulging forming, the dimension of forming zone in the middle of the die is enlarged from 68 mm to 80 mm, as shown in Fig. 11a. The simulation result in Fig. 11b shows a uniform thickness, the maximum thinning ratio of 16.5%, and no obvious wrinkling defects, indicating that the optimized mold and slow loading path can improve the part forming. Therefore, by adopting the slow gas loading path, the maximum thinning ratio reduces from 67.65% to 26.9%.

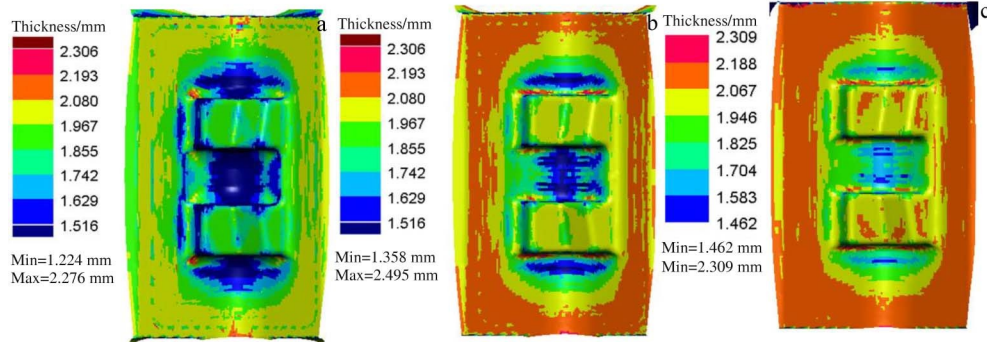


Fig.10 Simulation results with slow gas loading path at different temperatures: (a) 700 °C, (b) 750 °C, and (c) 800 °C

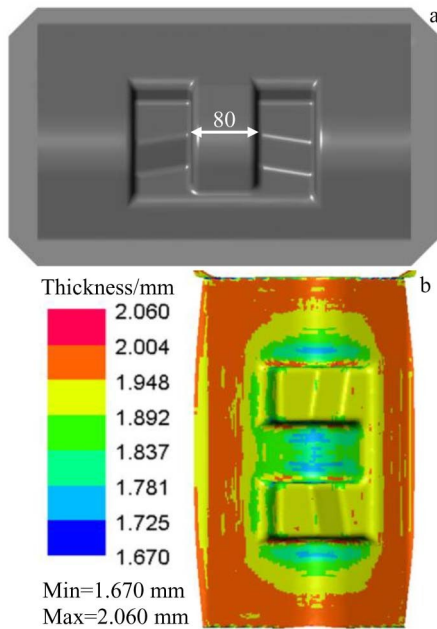


Fig.11 Schematic diagram of optimized die (a); simulation result of No.4 test using optimized mold (b)

Furthermore, increasing the gap between two parts within the mold leads to the further reduction in the maximum thinning ratio to 16.5%.

4 Experiment

4.1 Composite process of deep drawing and gas bulging

According to the finite element simulation results, the composite process of deep drawing and gas bulging was conducted with the process parameters of 800 °C, 80% of the part depth, 2.5 MPa, and slow gas loading path. After cleaning with alcohol, a special coating was sprayed on mold surface to prevent oxidization at high temperatures. After the mold was assembled into the heating furnace, the blank was heated and held at 800 °C for 15 min. The punch was modified to draw 80% of the depth of part. Subsequently, the gas bulging forming was conducted under program-controlled argon gas pressure. The experiment scheme and result are shown in Fig.12a and 12b, respectively.

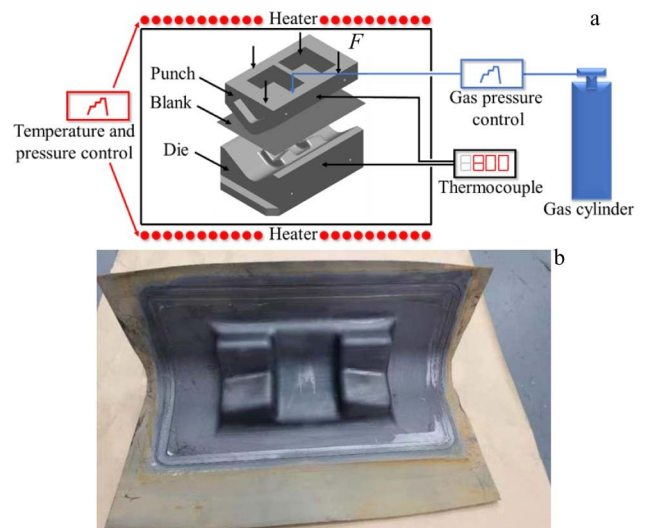


Fig.12 Schematic diagram of composite hot forming process (a); experiment result of composite hot forming process (b)

4.2 Forming accuracy

The accuracy analysis of formed part mainly involves the drawing depth and thickness^[25-26]. For the complex box part, it is necessary to measure the side height of the part. The friction between the material and the mold is very large during gas bulging forming, which causes uneven wall thickness. It is also necessary to measure the thickness at the part bottom close to the round corner. Since the forming part is actually two parts arranged side by side with the remaining material, the formed part is cut, trimmed, and ground to facilitate the measurement. The measuring points are selected at the side and bottom corners of the formed part to analyze the side height and wall thickness.

The measurement results of height and wall thickness are shown in Fig.13a and 13b, respectively. The minimum height of the part side is 20.1 mm, which allows sufficient cutting margin for subsequent trimming. The minimum wall thickness at measuring point 6 is 1.61 mm, and the maximum wall thickness at measuring point 12 is 1.75 mm. The thickness difference is 0.14 mm. The thickness distribution of the part is uniform, and the maximum thinning ratio is 19.55%, satisfying the forming accuracy requirements.

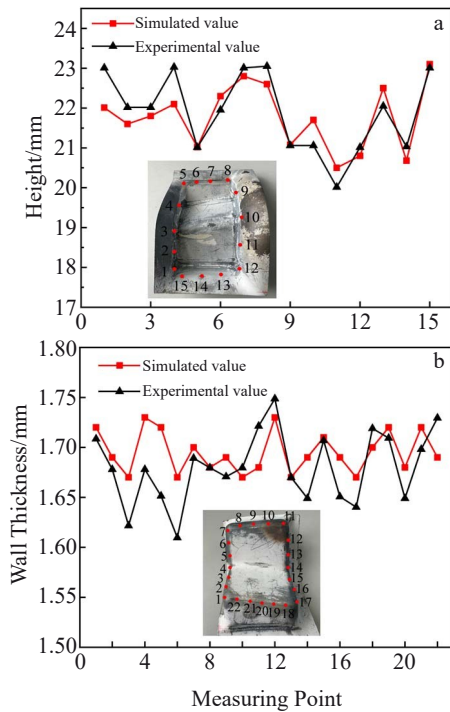


Fig.13 Measurement results of height (a) and wall thickness (b)

5 Conclusions

1) The deformation resistance of TC2 titanium alloy decreases and the elongation increases under the condition of high temperature and low strain rate, and the deformation is more uniform. The maximum elongation of 212.5% is obtained at 800 °C and 0.001 s⁻¹, which is the optimal forming condition for the complex box part.

2) The optimal deep drawing ratio should be 80%. A set of mold for the conduction of deep drawing and gas bulging can greatly simplify the process and improve the production efficiency.

3) The gas loading path exhibits the most significant influence on the simulated forming results. By adopting the slow gas loading path, the maximum thinning ratio reduces from 67.65% to 26.9%. Furthermore, increasing the gap between two parts within the mold leads to the further reduction in the maximum thinning ratio to 16.5%.

4) The maximum thinning ratio of the formed part is 19.55%, which is less than the accuracy requirement of 25%. The relative error with the simulated forming part is only 3.59%. The minimum height of the bottom surface of the part side is 20.1 mm after cutting, which is much higher than 18 mm. The composite hot forming process of deep drawing and gas bulging can be used to manufacture similar complex box parts.

References

1 Yin H L, Meng L J, Lu Y P et al. *Rare Metal Materials and*

Engineering[J], 2023, 52(3): 806

2 Du Bing, Li Yang, Zhao Chonghao et al. *Journal of Plasticity Engineering*[J], 2022, 29(10): 72 (in Chinese)

3 Tomáš M, Evin E, Kepič J et al. *Metals*[J], 2019, 9(10): 1058

4 Varandi A B. *Mechanics & Industry*[J], 2020, 21(1): 112

5 Liu Zhe, Wang Aiqin, Xie Jingpei et al. *Transactions of Materials and Heat Treatment*[J], 2021, 42(6): 22 (in Chinese)

6 Hassan S H A, Hossein M S S. *Proceedings of the Institution of Mechanical Engineers*[J], 2022, 236(6-7): 920

7 Wang K h, Liu G, Zhao J et al. *Journal of Materials Processing Technology*[J], 2017, 259: 387

8 Fu Kunming, Yang Xiaoke, Yang Bo et al. *Forging & Stamping Technology*[J], 2023, 48(5): 123 (in Chinese)

9 Xu Ye, Wang Guofeng, Lin Haipeng et al. *Journal of Plasticity Engineering* [J], 2021, 28(11): 8 (in Chinese)

10 Zhou Linghua, Shen Zhongwei, Xu Tao et al. *Forging & Stamping Technology*[J], 2022, 47(8): 76 (in Chinese)

11 Hu Zhiqing, Li Xinchun, Xi Jia et al. *Journal of Alloys and Compounds*[J], 2022, 911: 165055

12 Li Yong, Liu Junwei, Gao Wenliang et al. *Rare Metal Materials and Engineering*[J], 2022, 51(8): 2992 (in Chinese)

13 Zong Y Y, Shao B, Wang X G et al. *Advanced Engineering Materials*[J], 2018, 20(11): 1800690

14 Song F, Wang N, Chen M H et al. *Rare Metal Materials and Engineering*[J], 2022, 51(9): 3252

15 Lu Y P, Meng L J, Ying H L et al. *Rare Metal Materials and Engineering*[J], 2023, 52(3): 785

16 Kalienko M S, Volkov A V, Zhelnina A V et al. *Metal Science and Heat Treatment*[J], 2019, 61(5): 489

17 Yang S L, Liang P, Gao F Y et al. *Materials*[J], 2022, 16(1): 280

18 Yang Xingyuan, Jiang Muchi, Liu Yi et al. *Rare Metal Materials and Engineering*[J], 2023, 52(12): 4125 (in Chinese)

19 Zhao G L, Liu S Z, Zhang C et al. *Vacuum*[J], 2022, 197: 110841

20 Zhou Chi, Deng Junjie, Zhang Wentao et al. *Journal of Plasticity Engineering*[J], 2018, 25(4): 129 (in Chinese)

21 Zhang L Y, Liu H, Wang W Y. *Procedia Engineering*[J], 2017, 174: 524

22 Yu Zhengzhuo. *Forging & Stamping*[J], 2019, 44(20): 53 (in Chinese)

23 Qi Fei, Chen Dong, Li Huiyu et al. *Journal of Plasticity Engineering*[J], 2019, 26(3): 89 (in Chinese)

24 Zhu Lin, Xu Yong, Hu Shengshuang et al. *Rare Metal Materials and Engineering*[J], 2023, 52(5): 1819 (in Chinese)

25 Wan Miaomiao, Zhu Yingxia, Chen Rong et al. *Materials China*[J], 2023, 42(3): 266 (in Chinese)

26 Hong Quan, Guo Ping, Zhou Wei. *Titanium Industry Progress*[J], 2022, 39(5): 27 (in Chinese)

复杂盒形件拉深气胀精确热成形工艺

乔旭东, 陈明和, 谢兰生

(南京航空航天大学 机电学院, 江苏 南京 210016)

摘要: 针对复杂盒形零件一次拉深成形不足的问题, 提出了一种拉深气胀复合精确热成形工艺, 其成形零件的外形及壁厚均满足设计要求。以 TC2 钛合金复杂盒形件为研究对象, 研究了 TC2 钛合金在 550~800 °C 和 0.001~0.1 s⁻¹ 条件下的高温成形性能。设计了一套可一次性完成拉深、气胀的模具。基于有限元仿真模拟软件 PAM-STAMP 对零件成形过程进行模拟, 获得了优化工艺参数并进行实验验证。结果表明: PAM-STAMP 仿真软件可以预测零件拉深和气胀缺陷, 优化了工艺参数和模具形状并进行实验验证。实验在 800 °C、气体压力 2.5 MPa 条件下获得了壁厚、侧边高度均符合设计要求的零件, 验证了该拉深气胀复合工艺的可行性。

关键词: TC2 钛合金; 高温流变性能; 复合工艺; 数值模拟

作者简介: 乔旭东, 男, 1999 年生, 硕士生, 南京航空航天大学机电学院, 江苏 南京 210016, E-mail: xdqiao@nuaa.edu.cn